GAMMA-RAY COMPTON LIGHT SOURCE DEVELOPMENT AT LLNL

F.V. Hartemann#, S.G. Anderson, C.P.J. Barty, D.J. Gibson, C.A. Hagmann, M.S. Johnson, I. Jovanovic, D.P. McNabb, M.J. Messerly, J.A. Pruet, M.Y. Shverdin, C.W. Siders, A.M. Tremaine, LLNL, Livermore, CA 94550, U.S.A.

Abstract

A new class of tunable, monochromatic gamma-ray sources capable of operating at high peak and average brightness is currently being developed at LLNL for nuclear photo-science and applications. These novel systems are based on Compton scattering of laser photons by a high brightness relativistic electron beam produced by an rf photoinjector. Key technologies, basic scaling laws, and recent experimental results are presented, along with an overview of future research and development directions.

INTRODUCTION

Recent advances in high brightness rf gun and fiber laser technology have enabled the development of a new class of compact, tunable, narrow-bandwidth light sources capable of producing MeV photons with unprecedented brightness. Such new sources rely on Compton scattering of incident photons produced by a TW-class laser off a bright relativistic electron beam to generate Doppler-upshifted photons in a highly collimated beam. The main goal of this paper is to present a technical overview of so-called T-REX (Thomson-radiated extreme x-ray) sources and their key capabilities, and to provide an update on our progress.

COMPTON SCATTERING

Incident photons, with 4-wavenumber $k_\mu = (\omega_0 / c, \mathbf{k}_0)$, can Compton scatter off electrons with initial 4-momentum $m_0 c u_\mu$, to be Doppler-upshifted according to the Compton formula, which is derived from 4-momentum conservation: $\hbar k_\mu + m_0 c u_\mu = \hbar q_\mu + m_0 c v_\mu$, where q_μ is the 4-wavenuber of the scattered photon, and $m_0 c v_\mu$ is the electron 4-momentum after the interaction. This leads to:

$$\omega_x = \frac{\gamma\omega_0 - \mathbf{u}\cdot c\mathbf{k}_0}{\gamma + \lambda\!\!\!^{-}_C k_0 - \mathbf{n}_x \cdot \left(\mathbf{u} + \lambda\!\!\!^{-}_C \mathbf{k}_0\right)}. \quad (1)$$

Here, ω_x is the frequency of the scattered photon, and $\mathbf{n}_x$ is a unit vector in the direction of observation; $\lambda\!\!\!^{-}_C = \hbar / m_0 c$ is the Compton wavelength of the electron.

The differential cross-section for this process is described by the Klein-Nishina formula [2]. Limiting the expression to spin-unpolarized electron beams; introducing the classical electron radius, r_0; the incident and scattered light-cone variables $\kappa_0 = u_\mu k^\mu$ and $\kappa_x = v_\mu q^\mu$; and the incident and scattered 4-polarizations, ε_μ^0 and ε_μ^x, one obtains:

$$\frac{d\sigma}{d\Omega_x} = \frac{r_0^2}{2}\left(\frac{\omega_x}{\kappa_0}\right)^2 \left\{ \begin{array}{l} \frac{1}{2}\left(\frac{\kappa_0}{\kappa_x} + \frac{\kappa_x}{\kappa_0}\right) - 1 \\ +2\left[\begin{array}{l} \varepsilon_\mu^0 \varepsilon_x^\mu - \frac{\left(\varepsilon_\mu^0 u^\mu\right)\left(\varepsilon_\mu^x v^\mu\right)}{\kappa_0} \\ - \frac{\left(\varepsilon_\mu^x u^\mu\right)\left(\varepsilon_\mu^0 v^\mu\right)}{\kappa_x} \end{array} \right]^2 \end{array} \right\}. \quad (2)$$

The differential cross-section integrates to the well-known Thomson cross-section, $\sigma = 8\pi r_0^2 / 3$.

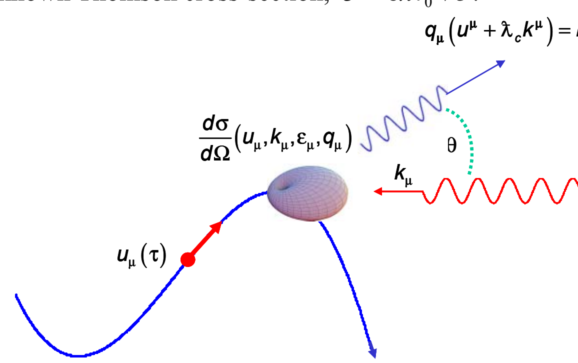

Figure 1: Schematic of Compton scattering

The brightness of Thomson scattering light sources was been studied theoretically [1] and computationally [3], and shown to scale favorably at high energy; this is due to the close correlation between the scattered light phase space and that of the incident electron beam: for a given normalized emittance, ε_n, the physical emittance of the electron beam scales as ε_n / γ; in turn, this implies that the scattered light is better collimated and has narrower bandwidth. For example, given the laser and electron beam parameters described in Table 1, the peak on-axis spectral brightness is shown in Fig. 2: the blue line corresponds to the analytical theory presented in Ref. [1], while the red squares are generated by a fully three-dimensional code that has been extensively benchmarked against a series of detailed experiments at LLNL [3]; the maximum brightness is shown to scale as $(\gamma/\varepsilon_n)^2$.

For narrow bandwidth operation, the difference between the Compton and Thomson scattering formalisms becomes significant: this is shown in Fig. 3, where the relative frequency difference is plotted as a function of the beam energy for an incident wavelength of 1064 nm; even for modest energies, recoil is sufficient to result in a frequency offset comparable to the scales of interest.

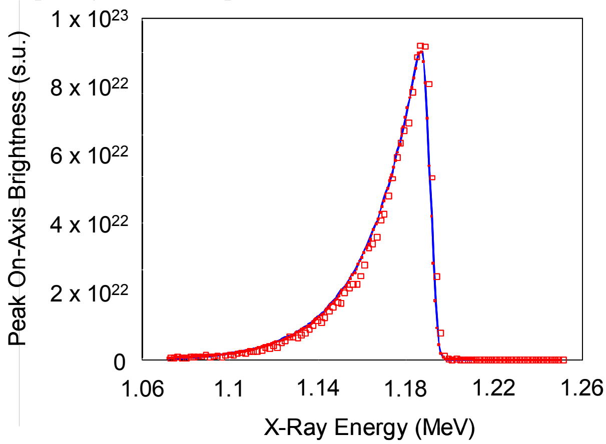

Figure 2: on-axis spectral brightness

Table 1: linac and laser parameters used for Fig. 2

	Linac	Laser
Particle energy	250 MeV	$\hbar\omega_0 = 1.24$ eV
Particle #	$q = N_e e = 1$ nC	$W = 1$ J
Pulse duration	$\Delta\tau/\sqrt{2} = 100$ fs	$\Delta t = 5$ ps
Focal spot radius	$r_b/\sqrt{2} = 10$ µm	$w_0 = 20$ µm
Energy spread	$\Delta\gamma/\sqrt{2}\gamma = 0.1\%$	$\Delta\omega = \sqrt{2}/\Delta t$
Transverse phase space (*rms*)	$\varepsilon_n = 1$ mm.mrad	$\Delta k_{\perp}/k_0 \ll 1$

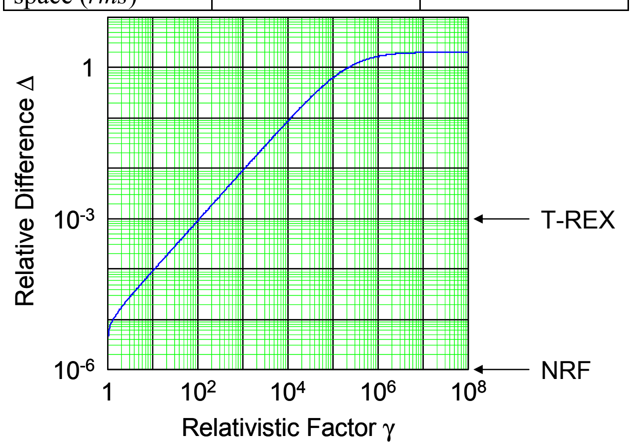

Figure 3: relative recoil frequency offset as a function of γ

LLNL T-REX SOURCE

A prototype T-REX source is currently under construction at LLNL; it is designed to perform proof-of-principle nuclear resonance fluorescence (NRF) imaging experiments at photon energies up to 700 keV [4]. The overall system architecture is shown in Fig. 4; key components include a high brightness S-band rf gun and associated fiber-based UV photocathode laser system, a 125 MeV linac, and a Joule-class, 10 Hz drive laser, with frequency tripling down to 355 nm. This source will produce 10^9 photons/shot; the effective γ-ray beam divergence will be 0.5 mrad; and its fractional bandwidth will be < 1%.

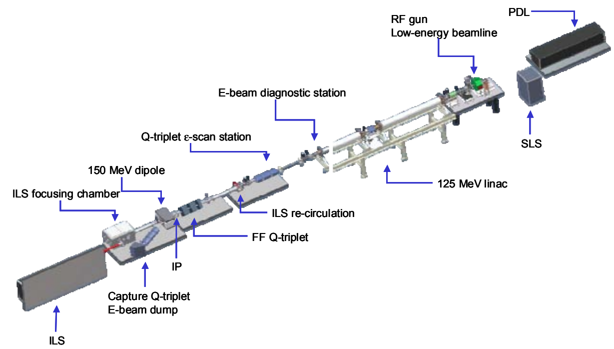

Figure 4: T-REX overall schematic

As indicated in the previous section, the x-ray phase space closely maps that of the electron beam; this implies that high charge, low emittance and low energy spread electron beams are critical to enable the development of high brightness Compton scattering light sources. Additional issues, such as the picosecond timing required between the electron and laser beams, also point in the direction of rf guns as the electron source of choice.

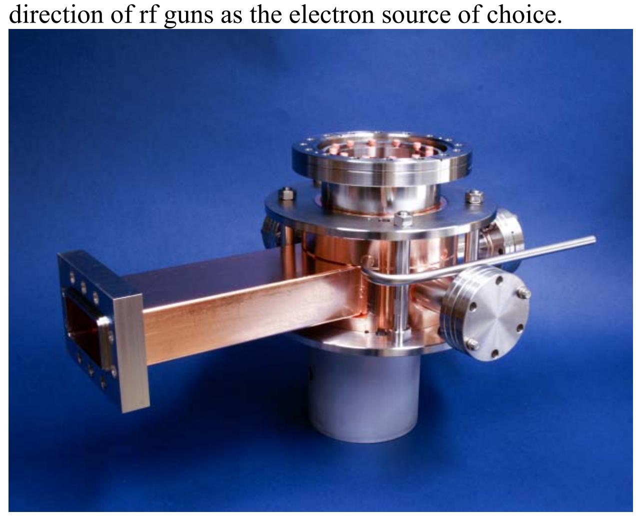

Figure 5: UCLA/LLNL S-band rf gun

One of the key characteristics of rf guns is the very high accelerating gradient under which the system operates: up to 120 MeV/m for good vacuum and processing conditions. This yields very bright photo-electron bunches that are naturally synchronized to the laser pulses used to illuminate the photocathode. However, to take full advantage of the unique properties of rf guns, one requires highly specific spatial and temporal laser pulse shapes at the photocathode, as shown in Fig. 6.

Given the stringent laser requirements for both the Thomson scattering drive laser and the rf gun photocathode illumination system, and the need for robustness, compactness, efficiency, and versatility, fiber-based systems are ideal candidates to meet the technical specifications of Compton light sources, especially in view of the fact that sputtered Mg can reduce the UV laser requirement down to a few tens or a few hundreds of μJ.

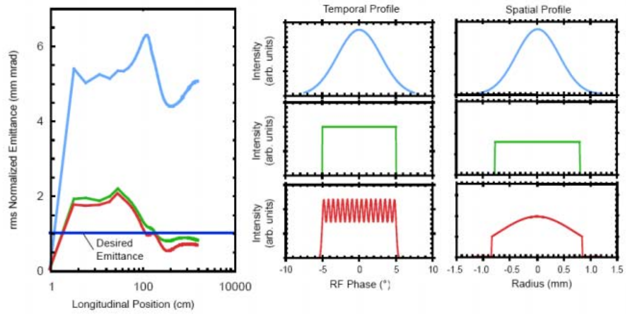

Figure 6: influence of the UV pulse shape on emittance

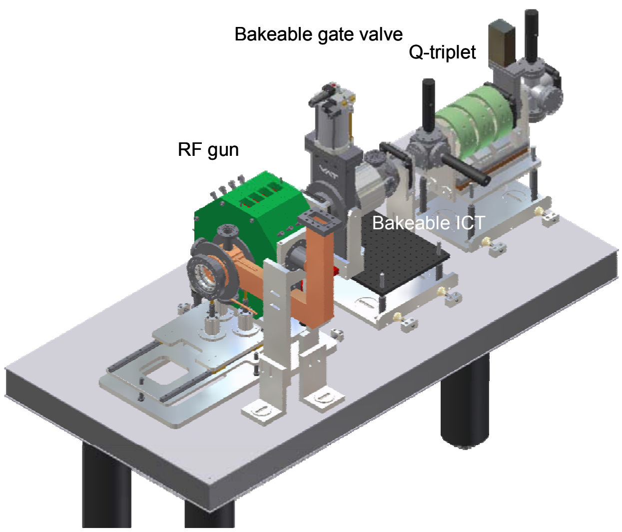

Figure 7: low-energy beamline

Such novel lasers are highly stable, in part because of diode pumping; integrated optics, including fiber switches and chirped fiber Bragg gratings allow for the production and manipulation of ultrashort laser pulses, with energies up to 1 mJ. Higher energies can be obtained by bulk amplification, while the fiber systems themselves are readily scaleable to multi-kW average powers. Moreover, using hyper-Michelson interferometers [5], it is possible to produce arbitrary and well-defined UV pulses (Fig. 8).

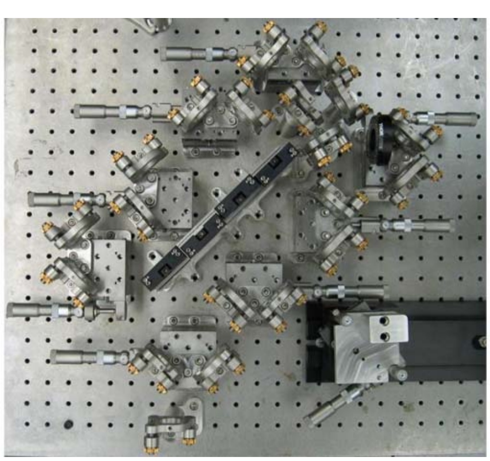

Figure 8: hyper-Michelson

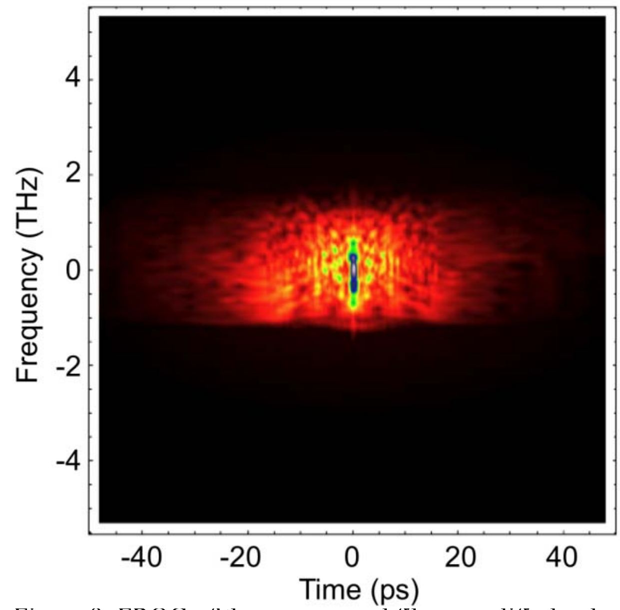

Figure 9: FROG of the compressed fiber-amplified pulse

In Fig. 9, the IR pulse produced by the fiber-based system is analyzed using frequency-resolved optical gating, prior to frequency-quadrupling and injection into the hyper-Michelson temporal shaper.

Finally, a 25 W (2.5 J at 10 Hz) Nd:glass amplification chain is used to produce the drive pulses at the interaction region; this system is driven by a common fiber laser oscillator to ensure the required sub-ps synchronization.

This work was performed under the auspices of the U.S. Department of Energy by University of California, Lawrence Livermore National Laboratory under Contract W-7405-Eng-48.

REFERENCES

[1] F.V. Hartemann, *et al.*, "High-energy scaling of Compton scattering light sources", Phys. Rev. STAB **8**, 100702 (2005).

[2] G. Bhatt, *et al.*, "Relativistic spin-dependent Compton scattering from electrons", Phys. Rev. **A28**, 2195 (1983).

[3] W.J. Brown, *et al.*, "Three-dimensional time and frequency-domain theory of femtosecond x-ray pulse generation through Thomson scattering", Phys. Rev. STAB **7**, 060702; "Experimental characterization of an ultrafast Thomson scattering x-ray source", *ibid* 060703 (2004).

[4] J. Pruet, *et al.*, "Detecting clandestine materials with nuclear resonance fluorescence", Jour. Appl. Phys. **99**, 123102 (2006).

[5] C.W. Siders, *et al.*, "Efficient high-energy pulse-train generation using a 2n-pulse Michelson interferometer", Appl. Opt. **37**, 5302 (1998).

